

A Study on the Circumferential Groove Effects on the Minimum Oil Film Thickness in Engine Bearings

Myung-Rae Cho*

Turbo & Power Machinery Research Center, Seoul National University

Hung-Ju Shin

Graduate School, Seoul National University

Dong-Chul Han

Professor, Mechanical Design & Production Engineering, Seoul National Univ

This paper presents the effects of circumferential groove on the minimum oil film thickness in engine bearings. The fluid film pressures are calculated by using the infinitely short bearing theory for the convenience of analysis. Journal locus analysis is performed by using the mobility method. A comparison of minimum oil film thickness of grooved and ungrooved bearing is presented. It is found that circumferential 360° groove only reduces the absolute magnitude of the oil film thickness, but 180° half groove affects the shape of film thickness curve and position of minimum oil film thickness.

Key Words : Groove, Minimum Oil Film Thickness, Engine Bearing, Mobility Method

Nomenclature

B	: Width of bearing [m]
B_g	: Width of groove [m]
C	: Clearance [m]
D	: Bearing diameter [m]
F_r, F_ϕ	: Fluid film force [N]
h	: Film thickness [m]
M_c, M_ϕ	: Mobility term
p	: Fluid film pressure [N/m ²]
R	: Bearing radius [m]
W	: Acting force [N]
z	: Axial coordinate [m]
ϵ	: Eccentricity
ϕ	: Attitude angle [rad]
φ	: Radial coordinate [rad]
η	: Viscosity [Pa · s]
ω_b	: Angular velocity of bearing [rad/s]
ω_j	: Angular velocity of journal [rad/s]
ω_L	: Angular velocity of load [rad/s]

$$\bar{\omega} = \frac{1}{2} \left[1 + \frac{\omega_b}{\omega_j} - 2 \frac{\omega_L}{\omega_j} \right]$$

1. Introduction

The performance of engine bearing plays an important role in the fuel economy and engine durability. In recent years, the tendency of engine design has been to achieve small size and low weight, but the power required in engine has been continuously increasing. According to these demands, the operating conditions of engine bearings have become very severe, and low viscosity engine oil is used to reduce the friction loss and improve the starting ability at low temperature. However, there are some problems such as breakdown of bearing due to rupture of the oil film and deterioration of engine efficiency caused by bearing damage. The investigation of MOFT (minimum oil film thicknesses) in engine bearing is important to prevent the above problems and improve their performance, and therefore, much research into the theoretical prediction (Booker, 1965, 1971, Goenka, 1984, Fantino et al., 1979, 1985, Cho et al., 1998(a), 1999(b)) and experi-

* Corresponding Author,

E-mail : engine@amed.snu.ac.kr

TEL : +82-2-880-1682 ; FAX : +82-2-885-8804

Turbo & Power Machinery Research Center, Seoul National University, San 56-1 Shillm-dong Kwanak-gu, Seoul 151-742, Korea. (Manuscript Received November 3, 1999; Revised April 11, 2000)

mental measurement (Bates and Benwell, 1988, Choi et al., 1992, 1993) for MOFT in engine bearing have been performed.

Engine oil has to be sufficiently supplied to the bearing for preventing the collapse of oil film. However it is not a fundamental means of solving the problems for the economical lubrication. Therefore most of the engine bearings adapt to the oil reservation groove as an alternative solution. The circumferential groove has some advantages for lubrication and cooling. However there are only a few research papers on the effect of circumferential groove on MOFT. Jones (1982) studied the effect of groove in engine bearing by considering oil film history, and Choi et al. (1992, 1993) measured the minimum oil film thickness in engine main bearing with circumferential half groove by using the total capacitance method, and then compared with theoretical results.

The aim of this paper is to investigate the effect of circumferential groove on MOFT. The oil film pressure is solved by using the short bearing theory, and the mobility method is used to obtain the trajectory of the journal center. From these, the effect of groove on the oil film thickness in engine bearing is presented in the form of MOFT curve.

2. Theory

The Reynolds equation in short bearing can be written as:

$$\frac{\partial}{\partial z} \left(h^3 \frac{\partial p}{\partial z} \right) = 12\eta \cdot \left(\frac{1}{C} \right)^2 [\dot{\epsilon} \cos \varphi + \epsilon \cdot (\dot{\phi} - \bar{\omega}) \cdot \sin \varphi] \quad (1)$$

The fluid film thickness is given by:

$$h(\varphi) = C(1 + \epsilon \cos \varphi) \quad (2)$$

The boundary conditions to solve the Eq. (1) are

$$\begin{aligned} &\text{at } z = \pm B/2, \quad p = 0 \\ &\text{at } z = 0, \quad \frac{\partial p}{\partial z} = 0 \end{aligned} \quad (3)$$

The fluid film pressure can be obtained by twice integrating Eq. (1) using the boundary

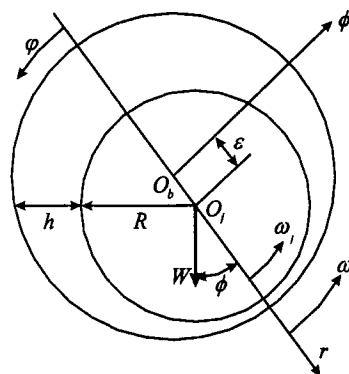


Fig. 1 Schematic diagram of a dynamically loaded journal bearing

conditions given above.

$$p(z) = \frac{6\eta C [\dot{\epsilon} \cos \varphi + \epsilon (\dot{\phi} - \bar{\omega})]}{h^3 [z^2 - (B/2)^2]} \quad (4)$$

The hydrodynamic force components due to the pressure distribution acting along and normal to the line of center (see Fig. 1) can be determined from:

$$F_r = - \int p \cos \varphi \cdot R \cdot d\varphi \cdot dz \quad (5)$$

$$F_\phi = \int p \sin \varphi \cdot R \cdot d\varphi \cdot dz \quad (6)$$

The equations of force equilibrium are given by:

$$W \cos \phi = F_r \quad (7)$$

$$W \sin \phi = F_\phi \quad (8)$$

By applying the mobility method to the Eq. (7) and Eq. (8), the following equations for the motion of journal center can be obtained (Booker, 1965, Taylor, 1993).

$$\dot{\epsilon} = \frac{W(C/R)^2}{\eta B D} \cdot M_\epsilon \quad (9)$$

$$\epsilon(\dot{\phi} - \bar{\omega}) = \frac{W(C/R)^2}{\eta B D} \cdot M_\phi \quad (10)$$

In Eq. (9) and Eq. (10), M_ϵ and M_ϕ are mobility terms, which can be written as:

$$M_\epsilon = \frac{(1 - \epsilon \cos \phi)^{3/2}}{\pi^2 (B/D)^2} \cdot [\pi \cos \phi \cdot (1 - \epsilon \cos \phi) - 4\epsilon \sin^2 \phi] \quad (11)$$

$$M_\phi = \frac{(1 - \epsilon \cos \phi)^{3/2}}{\pi^2 (B/D)^2} \cdot \sin \phi [4\epsilon \cos \phi + \pi(1 - \epsilon \cos \phi)] \quad (12)$$

From the assumed initial values of ϵ and ϕ , the

Table 1 Operating condition of test bearing

B/D	Con-Rod	Main
	0.39	0.33
Clearance	24 μm	11, 20, 23, 25 μm
rpm	3500, 5500	
Load Condition	Full load	
Viscosity	6.26cP	9.41cP

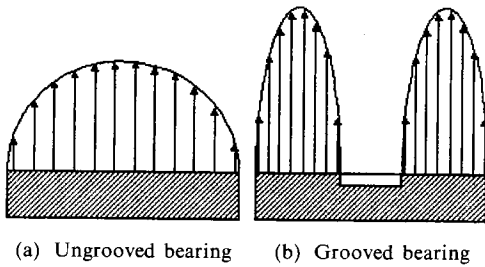


Fig. 2 Schematic diagram of axial pressure distribution

new values of eccentricity and attitude angle is obtained by the time integration of Eq. (9) and Eq. (10), and the time integration is repeated until the convergence for journal center trajectory is achieved.

When the journal center is located at the groove area, the oil film pressure is obtained at each of the two bearing sides except the groove. Figure 2 shows typical axial film pressure distribution in ungrooved and grooved bearings. In order to balance any given external load, the grooved bearing has higher maximum pressure than the ungrooved bearing.

3. Result and Discussion

Table 1 shows the operating condition and specification of test bearing.

The polar load diagrams for the connecting-rod bearing are displayed in Fig. 3. As shown in Fig. 3, as the engine speed increases the maximum load decreases, and the inertia force of the moving parts becomes more dominant than the explosive force of the cylinder gas. Maximum forces are 16.9kN and 12.1kN for 3500 rpm and 5500 rpm,

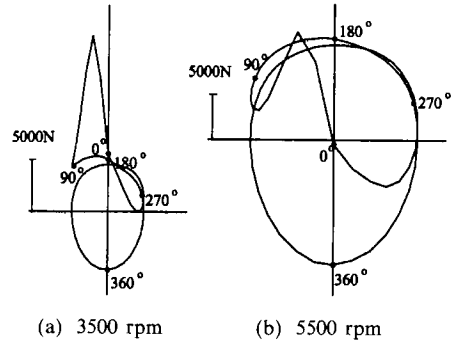
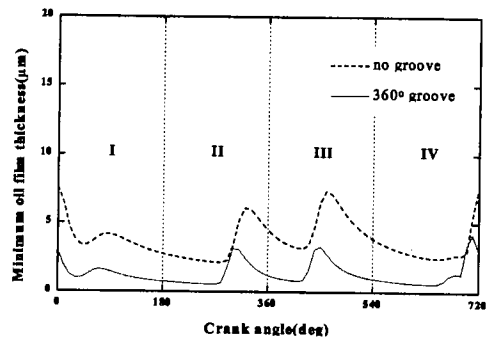
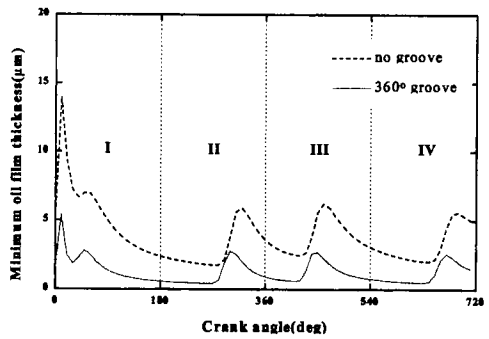


Fig. 3 Polar load diagrams for the connecting-rod



(a) 3500 rpm



(b) 5500 rpm

Fig. 4 Calculated results of MOFT curves in connecting-rod bearing ($B_g/B=0.25$)

respectively.

Figure 4 shows the effect of circumferential groove on the MOFT curve in the connecting-rod bearing. The Roman numerals (I , II , III , IV) represent the firing, exhaust, intake and compression strokes respectively. In the connecting-rod bearing, the 180° half groove is not considered because the bearing is rotating like a journal.

When comparing the two bearings, the shape of MOFT curves for 360° groove bearing is not changed but only the absolute magnitude of the film thickness decreases. The reduction of film thickness results from the decreasing load capacity caused by reduction of area to build up pressure. This result is similar to the effect of B/D on the film thickness. When the bearing width decreases, the minimum oil film thickness usually decreases as well (Cho et al., 1998(a)). The minimum oil film thickness of 2.11 μm in the case of using the ungrooved bearing is reduced to 0.54 μm at 3500 rpm, and 1.73 μm is reduced to 0.42 μm at 5500 rpm. However the minimum position of MOFT occurs during the exhaust stroke irrespective of engine speed variation.

In the case of highly loaded connecting-rod bearing, the groove is undesirable. Adapting 360° groove can reduce minimum oil film thickness by

a factor of two or more.

Figures 5, 6, 7, 8, and 9 show the effect of circumferential groove on the MOFT curve for main bearings. The resultant applied forces for the main bearings are presented in Fig. A1 (see Appendix). In the case of main bearings, the 180° half groove, which is circumferentially located at the upper bearing, is also considered. The absolute values and tendency of the MOFT in the 180° half and 360° groove bearings are somewhat different from those in the ungrooved bearing.

In the case of No. 2, No. 3, and No. 4 main bearings, there is a little change in the shape of MOFT curves between ungrooved bearing and 180° half groove bearing, and there is no change in the stroke where the minimum thickness occurs. However the absolute magnitude of the minimum film thickness is largely decreased in the case of 360° groove. Specially, in No. 1 main

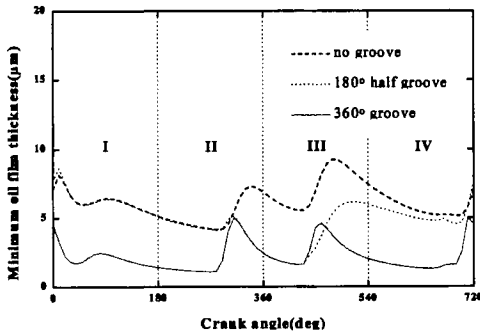


Fig. 5 Calculated results of MOFT curves in NO. 1 main bearing (3500rpm, $B_g/B=0.26$, $C=20 \mu\text{m}$)

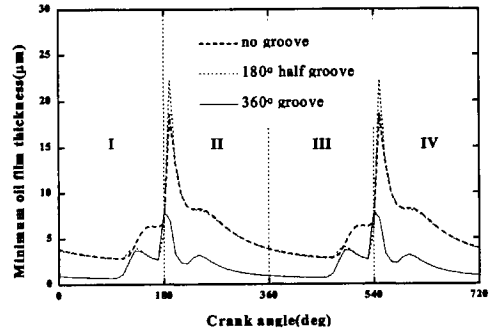


Fig. 7 Calculated results of MOFT curves in No. 3 main bearing (3500rpm, $B_g/B=0.26$, $C=25 \mu\text{m}$)

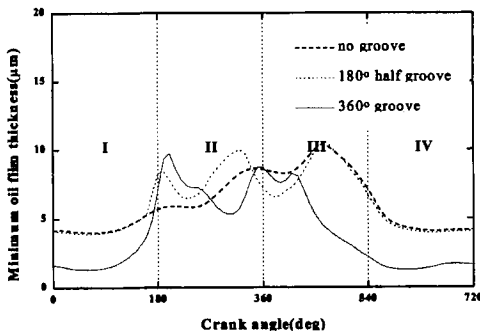


Fig. 6 Calculated results of MOFT curves in No. 2 main bearing (3500rpm, $B_g/B=0.26$, $C=11 \mu\text{m}$)

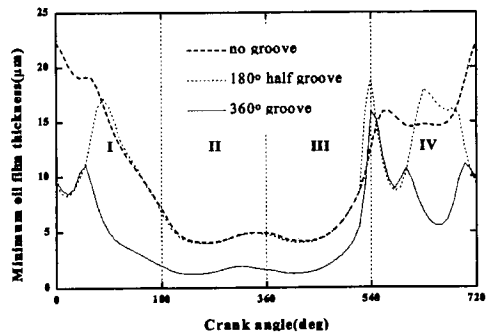


Fig. 8 Calculated results of MOFT curves in No. 4 main bearing (3500rpm, $B_g/B=0.26$, $C=23 \mu\text{m}$)

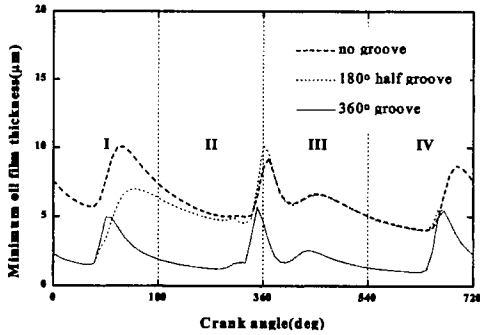


Fig. 9 Calculated results of MOFT curves in No. 5 main bearing (3500rpm, $B_g/B=0.26$, $C=25 \mu\text{m}$)

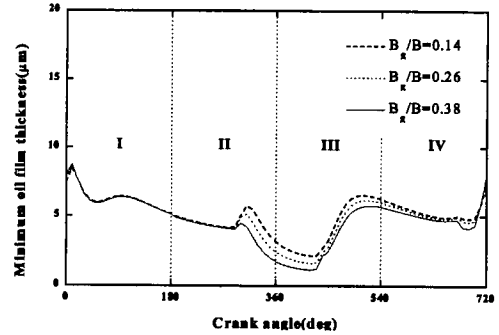


Fig. 10 Calculated results of MOFT for various groove widths in No. 1 main bearing (3500rpm, $C=20 \mu\text{m}$, 180° half groove)

bearing, the minimum position in the ungrooved and 360° groove bearing occurs during the exhaust stroke, but it occurs during the intake stroke in the case of 180° half groove. In No. 5 main bearing, the position is shifted from the compression stroke to the firing stroke.

In all engine main bearings, the 360° groove is undesirable because of severe reduction of MOFT during the whole engine cycle. Decreasing load carrying area reduces the load carrying capacity in the bearing. In No. 1, 3, and 5 main bearings, the 180° groove is not better than ungrooved bearing from the MOFT point of view. In No. 2, and 4 main bearings, the half groove reduces the MOFT at the relatively thick film thickness region. Therefore, in No. 2, and 4 main bearings, the half groove is recommended for the sufficient oil supply in spite of small change of MOFT.

Figure 10 shows the effect of groove width on the MOFT for No. 1 main bearing. As the width of the groove increases, the minimum value of MOFT decreases due to the reduction of pressure formation area. When the width of the groove is increased by twice, the minimum value of MOFT is reduced by 26% or so.

Figures 11 and 12 show the results of No. 1 and No. 5 main bearings at 5500 rpm. In the case of half groove, the position of MOFT is shifted in the same manner as in the case of 3500 rpm.

The expected values of MOFT for connecting-rod and main bearings are summarized in Table 2. In the case of 360° groove bearing, the decreasing rates of minimum thickness are about 68

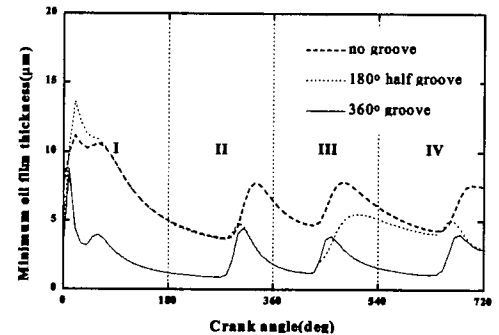


Fig. 11 Calculated results of MOFT curves in No. 1 main bearing (5500rpm, $B_g/B=0.26$, $C=20 \mu\text{m}$)

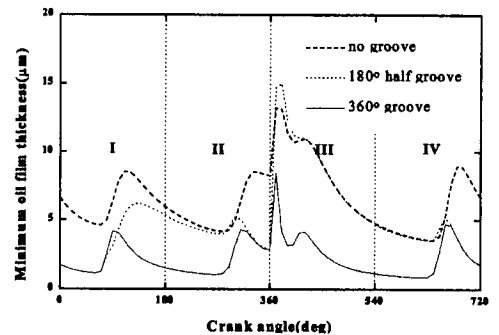


Fig. 12 Calculated results of MOFT curves in No. 5 main bearing (5500rpm, $B_g/B=0.26$, $C=25 \mu\text{m}$)

~76% in comparison with no groove, therefore all bearings have similar order of decreasing rate. However, in the case of 180° half groove, there are some differences in the decreasing rate according to the bearing number. The minimum film thick-

Table 2 Expected minimum oil film thickness (μm) in a connecting-rod and main bearings (3500 rpm)

	No groove	180° half groove	360° groove
Con-rod	2.11	-	0.54
Main 1	4.158	1.596	1.078
Main 2	4.0	3.9	1.28
Main 3	2.84	2.68	0.683
Main 4	4.06	3.98	1.25
Main 5	4.02	1.51	1.03

ness is reduced by 61% or so in the No. 1 and No. 5 main bearings, but the others are reduced only by about 2~6%.

4. Conclusion

The MOFT curve with consideration of circumferential groove is calculated by using the short bearing theory and mobility method. The following conclusions are derived.

(1) In comparison between ungrooved and 360° groove bearing, the shape of MOFT curve is almost unchanged, but the values of MOFT is largely reduced.

(2) In the case of 180° half groove located in the upper bearing, there are some differences in the values and shape of MOFT curve compared with ungrooved bearing. Specially, in the case of No. 1 and No. 5 main bearings, the minimum position of MOFT is shifted.

(3) The minimum value of MOFT decreases as the width of groove increases. When the width of groove is increased by twice, the minimum value of MOFT is reduced by 26% or so.

(4) It is thought that the 360° circumferential groove in the connecting-rod and main bearings is undesirable, because the MOFT is largely reduced during the whole engine cycle. In the case of 180° half groove, it is unprofitable in No. 1, 3, and 5 main bearings, but it is acceptable for the sufficient oil supply in No. 2, and 5 main bearings.

Acknowledgements

This work was carried out at the Turbo & Power Machinery Research Center in Seoul National University as part of G7 Project funded by the Korean Government. The authors are thankful for their continued support.

Reference

- Bates, T. W., and Benwell, S., 1988, "Effect of Oil Rheology on Journal Bearing Performance Part 3-Newtonian Oils in the Connecting-Rod Bearing of an Operating Engine," *SAE Paper No. 880679*.
- Booker, J. F., 1965, "Dynamically Loaded Journal Bearings: Mobility Method of Solution," *ASME Journal of Basic Engineering*, Vol. 87, No. 3, pp. 537~546.
- Booker, J. F., 1971, "Dynamically-Loaded Journal Bearings: Numerical Application of the Mobility Method," *ASME Journal of Lubrication Technology*, Vol. 93, No. 1 pp. 168~176.
- Cho, M. R., Jung, J. Y., and Han, D. C., 1998, "Analysis of Journal Locus in a Connecting Rod Bearing," *Journal of KSAE*, Vol. 6, No. 4.
- Cho, M. R., Han, D. C., and Choi, J. K., 1999, "Oil Film Thickness in Engine Connecting-Rod Bearing with Consideration of Thermal Effects: Comparison between Theory and Experiment," *ASME Journal of Tribology*, Vol. 121, pp. 901~907.
- Choi, J. K., Lee, J. H. and Han, D. C., "Oil Film Thickness in Engine Main Bearings: Comparison Between Calculation and Experiment by Total Capacitance Method," *SAE 922345*.
- Choi, J. K., Min, B. S. and Han, D. C., "Effect of Oil Aeration Rate on the Oil Film Thickness in Engine Bearings," *SAE 932785*.
- Fantino, B., Frene, J., and Du Parquet, J., 1979, "Elastic Connecting-Rod Bearing With a Piezoviscous Lubricant: Analysis of the Steady-State Characteristics," *ASME Journal of Lubrication Technology*, Vol. 101, pp. 190~200.
- Fantino, B., and Frêne, J., 1985, "Comparison of Dynamic Behavior of Elastic Connecting-Rod

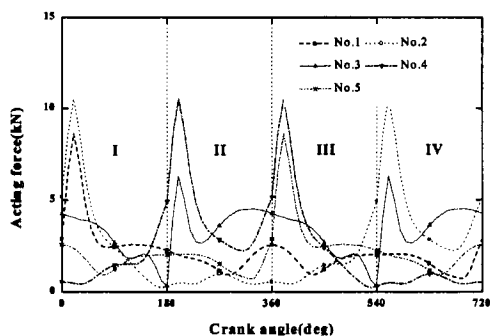


Fig. A1 Resultant acting forces on the main bearings (3500 rpm)

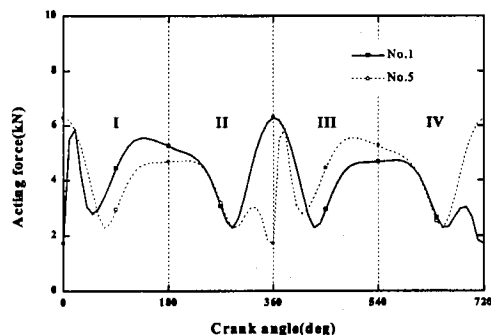


Fig. A2 Resultant acting forces on the main bearings (5500 rpm)

Bearing in Both Petrol and Diesel Engine," *ASME Journal of Tribology*, Vol. 107, pp. 87~91.

Goenka, P. K., 1984, "Dynamically Loaded Journal Bearings: Finite Element Method Analysis," *ASME Journal of Tribology*, Vol. 106, pp. 429~439.

Jones, G. J., 1982, "Crankshaft bearings: oil film history," *Proceedings, 9th Leeds-Lyon Symposium*, pp. 83~88.

Taylor, C. M., 1993, *ENGINE TRIBOLOGY*, Elsevier Science Publishers B. V., Amsterdam, pp.

89~112.

Appendix

Figure A1 and A2 show the acting forces on the main bearings at 3500 rpm and 5500 rpm respectively. There is no change in the absolute magnitude between No. 1 and No. 5, or No. 2 and No. 4, but only the load angle is changed. As the engine speed increases, the maximum load decreases, and the effect of explosive force is reduced.